More Electric Aircraft (MEA)

Scaling aspects and Weight impact

EMIL HOLMGREN

DHRUV HALDAR

Master's Programme, Aerospace Engineering, 120 credits
Date: January 29, 2021
Supervisor: Andreas Johansson,
andreas.x.johansson@saabgroup.com
Examiner: Lina Bertling Tjernberg, linab@kth.se
School of Electrical Engineering and Computer Science
Swedish title: Mer Elektriskt Flyg
Swedish subtitle: Skalningsaspekten och Viktpåverkan

More Electric Aircraft (MEA) / Mer Elektriskt Flyg

Abstract

This Thesis in Master of Science is about investigating fuel consumption of conventional and electrical types of subsystems on passenger aircrafts. The goal is to attain a tool that can help evaluate fuel consumption of airliners, both conventional and More Electric Aircrafts (MEA), for any given size and any given flight.

A similar study has been done on a passenger aircraft with comparable size to the Airbus A320 and this work is partly based on that study. The main differences to prior work are the added effects of weight impact and the passenger scaling aspect, to increase the accuracy and diversity of the model. Both effects are based on studies of existing technology for several airliners from Airbus and Boeing. Additional focus has been put on the largest secondary power consumers, such as the Environmental Control System (ECS) and the Ice Protection System (IPS). These systems were therefore investigated in detail.

Numerical models of passenger aircrafts were constructed, in MATLAB, with different levels of electrification and technologies. A special case were studied, simulations with an Airbus A320 for a round trip between Copenhagen and Stockholm on a hot day.

A summary of the result can be seen in table 1.

Table 1 – Fuel consumption comparison for Airbus A320 with 180 seats on a round trip between Copenhagen and Stockholm (1100 km) on a hot day.

Aircraft type	Total [kg]	Efficiency [kg/seat km]	Fuel savings [%]
Conventional	5311	0.0268	
Bleedless config. 1	5003	0.0253	5.8
Bleedless config. 2	4936	0.0249	7.1

For the Ice Protection System (IPS), the study provides a method for calculating the mass of ice formed when Airbus A320 aircraft is subject to in-flight icing conditions, which consist of the following:

- There is humidity due to clouds and precipitation.
- Air temperatures lie in the freezing range of 0 to -20°C.

Since icing cannot happen on a hot day, the study modifies the existing case by providing an icing air temperature of -17,15°C and an icing duration of 500 seconds. The methodology offers an option for automation of the simulation using IronPython programming.

Keywords

More Electric Aircraft (MEA), Fuel consumption, Weight, Scaling, Airbus A320, FENSAP-ICE, IPS, IronPython, ANSYS SpaceClaim, Icing, Meshing.

Sammanfattning

Sammanfattning på svenska.

Nyckelord

Mer Elektriskt Flyg, Bränsleförbrukning, Vikt, Skalning, Airbus A320, FENSAP-ICE, IPS, IronPython, ANSYS SpaceClaim, Nedisning, Meshning.

Acknowledgments

We would like to thank our supervisor Andreas Johansson and professor Lina Bertling Tjernberg, for all the guidance and encouragements. Finally, we would like to thank our families for their love and support, making it possible to conduct this research.

Stockholm, January 2021
Emil Holmgren and Dhruv Haldar

Contents

List of Figures

List of Tables

Listings

List of acronyms and abbreviations

HEPA High-Efficiency Particulate Air

HPC High-Pressure Compressor

LPC Low-Pressure Compressor

LoD Lift-to-Drag ratio

PHx Primary Heat Exchanger

PRV Pressure Regulator Valve

RHx Reheat Heat Exchanger

RP Rated Power

SHx Secondary Heat Exchanger

SP Specific Power

TSFC Thrust Specific Fuel Consumption

WE Water Extractor

kp Shaft Power Factor

ACM Air Cycle Machine

E-ACM Electric Air Cycle Machine

E-VCM Electric Vapour Cycle Machine

ECS Environmental Control System

MVD Median Volumetric Diameter

VCM Vapour Cycle Machine

Chapter 1

Introduction

With the rising number of flights around the world, the quest for increasing efficiency of aircrafts has become paramount, not only for economy but also for the environment. As conventional systems have largely reached there technological saturation and the power electronics are evolving in a higher pace, to move forward, engineers are beginning to look at electrical subsystems for the aircraft.

Examples of More Electric Aircrafts (MEA) are Boeing 787 Dreamliner, with no-bleed systems, and Airbus A380, with a combination of hydraulic and electric actuators.

To help decide, whether it is worth to invest in a novel system or not, a tool has been conceived to calculate the fuel consumption for several different subsystems, both conventional and electrical, for any given flight and for any commonly known airliner size.

The thesis begins with a description of the conventional airliner, the subsystems and the power distribution. Then, the individual subsystems are outlined together with the power consumption.

Due to time constraints, only the subsystems that consume most energy have been modelled in detail. Other subsystems are included in the model, but not described in same refinement.

The numerical model is then tested with a case study, the A320 on a round trip between Copenhagen and Stockholm. Also the pax-scaling effect is investigated for 15 different airliners, ranging from 156 passengers to 700 passengers. For the Ice Protection System (IPS), the existing case study is modified to relevant icing parameters.

Finally, the result is presented and discussed followed by conclusion and recommended future work.

1.1 Background

More Electric Aircraft technologies aim in reducing greenhouse gas emissions to make local and global air transport easier (Naayagi, 2013), while at the same time being cost-effective, reliable and promoting the production of more energy-efficient vehicles. Since the global population is rising, the number of people travelling around the world is also increasing. The rise in air travel drives the aviation industry to produce more vehicles which are energy efficient.
insert references.

The Advisory Council for Aeronautics Research in Europe has set several targets to be accomplished by 2050 for air transport (Darecki Marek, et al., 2012). Some of the goals proposed are 75% reduction in carbon dioxide (CO_2) emissions per passenger kilometre, a 90% reduction in nitrogen oxide (NO_x) emissions and perceived noise emittance of aircraft by 65% by 2050 (Darecki Marek, et al., 2012).

Swedavia, which forms the owns and operates Sweden's busiest airports (Swedavia - Wikipedia, n.d.), proposed a new aviation strategy in 2020 which focuses on the development of electric and more-electric architectures and the required necessary infrastructure by 2025 (Swedavia launches electric aviation strategy – Åre Östersund ready for first electric aircraft in autumn 2020 (About Swedavia, 2020). Swedish Climate Policy Framework establishes the implementation of zero net emissions of greenhouse gases into the atmosphere by 2045 (The Swedish climate policy framework, 2017). The government and corporate policies described above put confidence in the utilization of MEA Technologies.

1.2 Problem

What is the fuel consumption of aircrafts with different levels of electrification? Is the weight penalty going to eliminate the positive effect of higher efficiency for novel subsystems? How does the pax-scaling affect the overall efficiency of the aircraft?

Fuel consumption for an aircraft is a product of many things. It generally depends on technology, scale, flight conditions and duration.

Subsystems may differ in technology, efficiency, power management, weight and drag. Since every subsystem on an aircraft are connected and affecting each other in many ways, it is not clear if one system is better than

the other.

The pax-scaling effect, the aircraft size, is thought to influence the overall efficiency of the aircraft. This must be investigated.

Flight conditions, such as ambient temperature, air moisture content, speed and altitude should have an impact on fuel consumption.

To understand how everything affect the fuel consumption, detailed energy-models for every subsystem must be made. When all the subsystems are described along with the flight dynamics, a simulation for the complete aircraft can be made for a given flight profile, to obtain the total fuel spent on a flight.

By combining different subsystem technologies and various levels of electrification, multiple virtual aircrafts can be simulated and compared.

1.2.1 Scientific and engineering issues

Since this research is based on publicly available data, the availability and credibility of data is a core issue as it forms the input parameters for the numerical model.Much time has been spent on gathering and verifying data.

For the IPS system, verifiable detailed icing data is only available for a specific NACA Airfoil called NACA 0012. For proprietary reasons, the wing geometry data is not available. NACA 24012 is the assumed Airfoil for Airbus A320.

1.3 Purpose

The obvious purpose of this Master Thesis is that it provides an opportunity to display the knowledge and capability required for independent work as a Master of Science in Engineering.

The other purpose is to help mankind reducing environmental footprint on earth, while maintaining the ability to travel and transport goods.

1.4 Goals

The goal of this project is to compare fuel consumption of conventional and More Electric Aircrafts. This has been divided into the following three sub-goals:

1. Conceive a model that can predict the fuel consumption of passenger aircrafts with different subsystems, both conventional and electrical.

The model should be able to handle aircrafts of varying sizes, different routes and flight conditions.

2. The model should be able to support in the decision makings, whether it is worth to invest in a novel subsystem or not.

3. Gather publicly available knowledge into one place, that is relevant for fuel consumption calculations of passenger aircrafts, paving the way for further work in the subject.

1.5 Research Methodology

The research methodology is based on literature studies of publicly available sources. Data and knowledge has be gathered from several authors and compared against one another, to test the validity.

1.6 Delimitations

The study is based on 15 common airliners, ranging from 156 seats to 700 seats. A list of aircrafts that are in the study is shown in table XX. For simplicity, all the seats are assumed to be occupied, thus number of seats equals number of passengers (pax). In reality the passenger load factor for airliners is on an average around 80%, which means that every seat holds approximately 0.80 pax.

Due to time constrain, only one engine is modelled, the CFM56-5B, to calculate the bleed-air temperature. This engine is commonly equipped on the A320, our baseline airliner and is numerically scaled to fit all the other aircrafts. For airliners with other engines, this model can be misleading for the bleed system to some degree, due to different characteristics between engines.

Although many subsystems are included in the model, only the Environmental Control System (ECS) and Wing Ice Protection System (WIPS) are focused on in this thesis. Cowl Ice Protection is explained but not implemented in the simulations.

1.7 Structure of the thesis

Fill in all the chapters.

Chapter 2 presents the Environmental Control System (ECS), both bleed-air and electric systems. Chapter 4 presents the Ice Protection System (IPS), both bleed-air and electric systems.

Chapter 2

Environmental Control System

The main focus of this chapter is to give the reader an understanding of the Environmental Control System (ECS) on airliners, what it does, and what affects its power consumption. We will begin with the function of the ECS and explain why it is needed. Then the thermodynamic model, weight impact, and drag will be shown. Finally, shaft power and fuel consumption will be calculated.

2.1 ECS Function

The passenger aircraft is a closed environment, protecting what's inside against harsh conditions in the atmosphere. Depending on location and altitude, temperature outside can be higher than 30 °C or well below -50 °C, while the atmospheric pressure can be lower than that on the top of Mount Everest. The ECS is responsible for maintaining a pleasant temperature, healthy pressure and good air quality in the cabin. In this model the cabin temperature is set to 22 °C and the cabin pressure follows a cabin altitude scheme that corresponds to static pressure from sea level up to 2400 m, see figure A.1.

2.2 ECS Types

The core part of the ECS is called the air-conditioning pack. The air-conditioning pack is a refrigeration system that, conventionally, is driven by pressurized air, taken from the engine. For redundancy, there are at least two packs and they are mostly placed in the wing-body fairing under the fuselage, see figure 2.1.

Three different types of ECS-packs will be laid out:

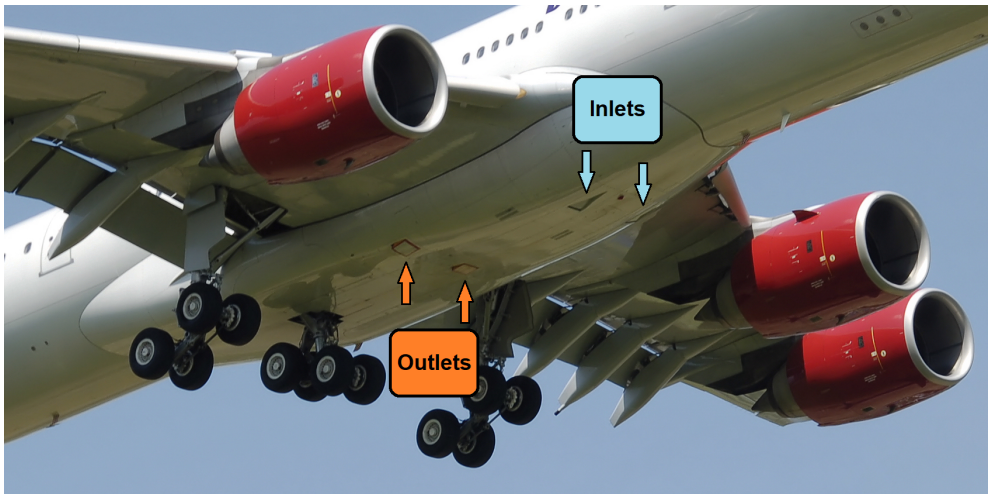

Figure 2.1 – Airbus A340-600 two ECS packs in the wing-body fairing with adjustable inlets and outlets for cooling air. Amended from Wikipedia.

1. The conventional, bleed-air driven, Air Cycle Machine (ACM).
2. The Electrical Air Cycle Machine (E-ACM).
3. The Electrical Vapour Cycle Machine (E-VCM).

2.2.1 Conventional Air Cycle Machine (ACM)

The conventional Air Cycle Machine (ACM), see figure 2.2, which is most commonly used, is driven by compressed air, called bleed-air, taken from the compressor stages in the engine core. The bleed-air, provide power to run the ACM and air for the cabin. Using the passing through air as a refrigerant, with a combination of turbine, compressors, valves, heat exchangers and outside air to dispense heat, the hot and compressed air can be cooled down well below freezing conditions.

Pressure and temperature of the bleed-air varies with thrust setting of the engine. An engine that is working hard gives bleed-air with high pressure and temperature. Here, the bleed-air can be tapped at either the Low Pressure Compressor (*LPC*) or at the High Pressure Compressor (*HPC*), depending on which port that can deliver just enough pressure to drive the ACM. Most of the time, when thrust is on a moderate level, bleed-air is tapped from the *HPC*. During short periods of time with high thrust setting, such as during takeoff, bleed-air is taken from the *LPC*. A Pressure Regulator Valve, *PRV*, is used the reduce the pressure to approximately 200 kPa.

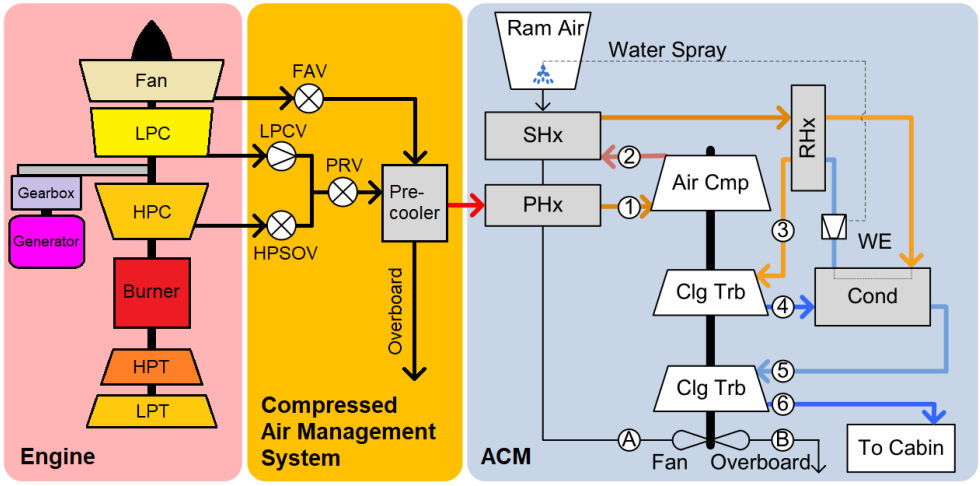

Figure 2.2 – Pneumatic Four-Wheel Condensing Air Cycle Machine. Amended from Parrilla, 2014, [1].

Typical bleed-air temperature for the simulated A320 is around 260 °C during cruise and at maximum around 340 °C during climb, which corresponds to bleed-air pressures around 400 kPa and 800 kPa respectively. For safety reasons, the bleed-air is cooled down below autoignition temperature (200 °C) of jet fuel, before it leaves the engine. Heat is dumped overboard with compressed air from the engine fan through the pre-cooler.

Before entering the Air Cycle Machine, the relatively hot airflow through a catalytic converter that breaks down ozone. Air enters the ACM through the Primary Heat Exchanger, *PHx*, then it is compressed. The heat is squeezed out and discarded through the Second Heat Exchanger, *SHx*. To prevent ice build-up in the system, moisture must be extracted from the air. To do this, some heat in the air is stored in the Reheat Heat Exchanger, *RHx*. While further cooling is done in the Condenser, droplets of water forms and gets expelled in the Water Extractor, *WE*. Extracted water can then be used to spray over the Secondary Heat Exchanger to increase its effectiveness. The dry and cold air can now regain the heat that has been stored earlier in the *RHx*. Finally, the air is expanded through a couple of Cooling Turbines, Clg Trb. The expansion extracts power from the compressed air to drive the ACM. After this stage, the temperature of the air can be as low as -18 °C.

To adjust the air temperature, hot air can be taken directly after the *PHx*, at point 1, through a bypass valve and is joined at point 6, where hot and cold air are mixed together. With this adjustment, the air from the ACM can have a temperature from -14 °C to 120 °C (Merzvinskas et al., 2020,

[8]). Before flowing to the cabin, fresh air from the ACM is mixed with recirculated air from the cabin. The mixing ratio is typical 50% fresh air and 50% recirculated air. A *HEPA*-type filter is used to capture most particles, bacteria, and viruses in the recirculated air. The fresh, clean air then makes its way to the cabin through the distribution network, and by the time it enters the cabin, its temperature can vary between 4 °C and 71 °C.

Air pressure in the cabin is maintained and regulated through one or two Out-Flow Valves, OFV, located at the bottom rear of the fuselage.

2.2.2 Electric Air Cycle Machine (E-ACM)

Taking the Conventional Air Cycle Machine, replace the bleed-air with pressurized air from electrically driven compressors, we get the Electric Air Cycle Machine (E-ACM), see figure 2.3. The main advantage over the bleed version is improved control over the pressure of the compressed air, as it is not relying on the thrust setting of the engine. Just enough pressure is produced to drive the ACM, about 100 kPa above cabin pressure.

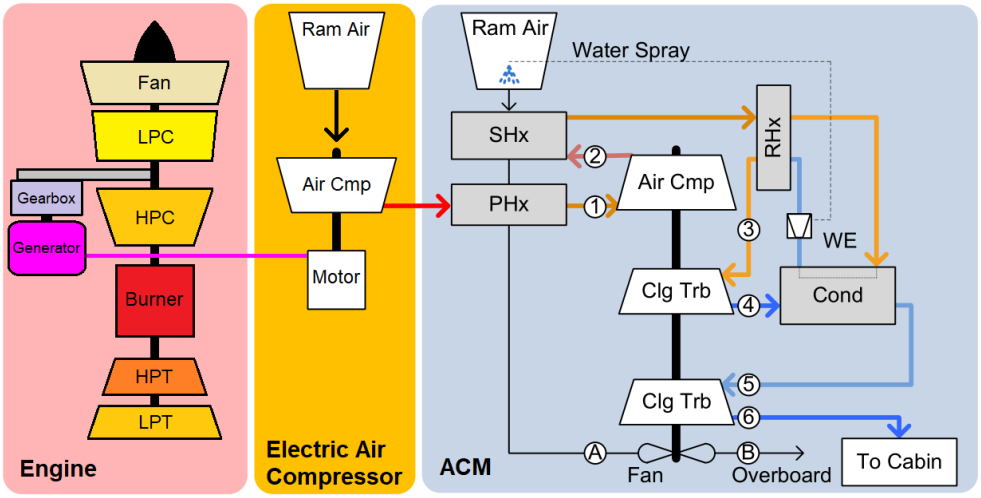

Figure 2.3 – Electric Four-Wheel Condensing Air Cycle Machine. Amended from Parrilla, 2014, [1].

2.2.3 Electric Vapour Cycle Machine (E-VCM)

The working fluid in the Electric Vapour Cycle Machine, E-VCM or even shorter VCM, is a refrigerant with greater thermodynamic properties than air. This means that the VCM is more efficient at cooling than the ACM. See figure

2.4. Fresh air for the cabin must still be compressed, but at a lower pressure, around 20 kPa above the cabin pressure. Thus less heat must be extracted and less power is required. Though, the E-VCM is more energy efficient than E-ACM, the fuel savings may not make up for other disadvantages, such as lower reliability and higher maintenance requirements.

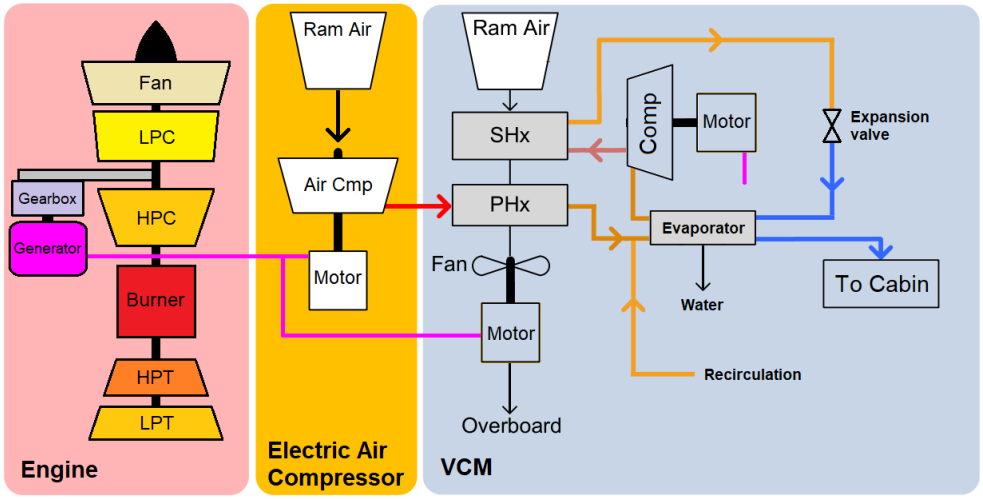

Figure 2.4 – Electric Vapour Cycle Machine. Amended from Parrilla, 2014, [1].

2.3 ECS Thermodynamics

Describe the thermodynamics for all 3 ECS variants. Energy balance.

What affects power consumption. Internal and external thermal loads. All assumed parameters.

bleed-air mass flow rate. Dependence of bleed temperature.

Include picture.

The most important parts of the thermodynamic of this model will be shown here in this chapter. How the model works in detail, can be seen in the Appendix A.2, where the MATLAB code is shown. The control volume of the thermodynamic model is the fuselage of the airliner. It is approximated as a cylinder with an effective length and diameter. The size of the fuselage is a function of pax. The thermal conductivity of the fuselage skin is assumed to have an average value of 5 W/m^2K (Chakraborty et al., 2016, [7]). There are

three ways for the heat to flow in and out of the cabin: through fresh air from the ECS, through the fuselage skin and internal heat generation.

2.3.1 Conventional Air Cycle Machine Thermodynamics

To maintain a cabin temperature of 295.15 K (22 °C) under various conditions, the ECS will initially adjust the temperature of the fresh air. If adjusting the fresh air temperature is not enough, then the airflow rate can be increased. According to regulations, the minimum amount of fresh outside air that must enter the cabin is 10 cfm/pax, which is equal to 6 g/paxs at standard sea level.

Thermal equilibrium for a hot day and static on ground can be described with:

$$\dot{Q}_{ECS} + \dot{Q}_{shadow} + \dot{Q}_{sun} + \dot{Q}_{pax} = 0 \tag{2.1}$$

,where

$\dot{Q}_{ECS}$	heat flux from the ECS
$\dot{Q}_{shadow}$	heat flux through the fuselage in shadow
$\dot{Q}_{sun}$	heat flux through the fuselage in the sun
$\dot{Q}_{pax}$	passenger associated heat flux

Heat flux from the ECS can be defined as:

$$\dot{Q}_{ECS} = \dot{m}_{air} C_p (T_{ECS} - T_{cabin}) \tag{2.2}$$

, where $\dot{m}_{air}$ is the air mass flow rate, C_p is specific heat capacity of air, T_{ECS} is air temperature provided by the ECS and T_{cabin} is cabin temperature.

Heat flux through the part of fuselage, that is in shadow, from ambient air is:

$$\dot{Q}_{shadow} = U(A_{wet} - A_{proj})(T_{amb} - T_{cabin}) \tag{2.3}$$

, where U is thermal conductivity of fuselage skin, A_{wet} is wet surface area of the fuselage, A_{proj} is projected area of the fuselage, T_{amb} is ambient temperature and T_{cabin} is cabin temperature.

Heat flux through the part of fuselage, that is in the sun can be expressed as:

$$\dot{Q}_{sun} = U A_{proj}(T_{amb} + \Delta T_{solar} - T_{cabin}) \tag{2.4}$$

, where ΔT_{solar} is the average temperature rise of the surface, due to solar radiation. The temperature rise is approximately 10 K (Cottony et al, 1941), for a white surface.

The passenger associated heat flux, $\dot{Q}_{pax}$, is based on metabolic heat and all other facilities such as entertainment, lighting, galley etc. It is roughly 190 W/pax (Slingerland et al. [9]).

Fresh Air Mass Flow Rate

Solving for the air mass flow rate, for on ground conditions, gives:

$$\dot{m}_{air,static} = \frac{U(A_{wet} - A_{proj})(T_{amb} - T_{cabin}) + U \cdot A_{proj}(T_{amb} + \Delta T_{solar} - T_{cabin}) + \dot{Q}_{pax}}{C_p(T_{cabin} - T_{inlet})} \tag{2.5}$$

, where cooling is assumed with $T_{inlet} = 259.37$ K (-13.8 °C), for a hot day.

When flying, assume that forced convection will remove most of the solar heating. The temperature rise due to solar heating will then be relatively small and can be neglected. The ambient temperature, T_{amb}, is replaced with total temperature, T_{total}, to include the kinetic heating effect, thus the air mass flow rate can be calculated as:

$$\dot{m}_{air,fly} = \frac{U \cdot A_{wet}(T_{total} - T_{cabin}) + \dot{Q}_{pax}}{C_p(T_{cabin} - T_{inlet})} \tag{2.6}$$

If heating is required (if eq. 2.5 or 2.6 gives negative value), then assume heating with $T_{inlet} = 393.15$ K (120 °C).

Ensure that the fresh air mass flow rate meets the regulation. If the calculated air mass flow rate is smaller than the minimum value, $\dot{m}_{air,min} = 0.006 \cdot pax$ kg/s, then set $\dot{m}_{air} = \dot{m}_{air,min}$.

With regulated air mass flow rate, a new inlet temperature must be calculated:

$$T_{inlet} = T_{cabin} - \frac{U \cdot A_{wet}(T_{tot} - T_{cabin}) + \dot{Q}_{pax}}{C_p \dot{m}_{air,min}} \tag{2.7}$$

Heat Exchangers

Excessive heat is expelled through the pre-cooler and heat exchangers in the ACM. The air mass flow rate through a heat exchanger is calculated with the

simple assumption that the difference of temperature between the hot air inlet and the cold air outlet is ΔT_{hx}. Further, assume adiabatic process that no heat is transferred to the environment, except between the air in the heat exchanger itself. If cooling of bleed-air is needed ($T_{bleed} > T_{safe}$), then the fraction of fan air and bleed-air mass flow rate can be expressed as:

$$\xi_{fan} = \frac{\dot{m}_{fan}}{\dot{m}_{air}} = \frac{T_{bleed} - T_{safe}}{(T_{bleed} - \Delta T_{hx}) - T_{fan}} \tag{2.8}$$

, otherwise $\xi_{fan} = 0$.

The fraction of cooling air flow through the heat exchangers in the ACM is expressed as:

$$\xi_{hx} = \frac{\dot{m}_{hx}}{\dot{m}_{air}} = \frac{T_{safe} - T_{shx}}{(T_{safe} - \Delta T_{hx}) - T_{tot}} \tag{2.9}$$

Conventional Air Cycle Machine Shaft Power

For bleed-air, shaft power is a function of air mass flow rate and bleed temperature. According to (Slingerland et al., 2007, [9]) the amount of exergy (in this case, shaft power), extracted from the engine, can be calculated by using:

$$Exergy = P_{shaft} = \dot{m}_{air} \left[(h - h_0) + T_0 \cdot (s - s_0) \right] \tag{2.10}$$

,where

P_{shaft}	shaft power
$\dot{m}_{air}$	bleed-air mass flow rate
h	enthalpy of bleed-air
h_0	enthalpy of air at compressor inlet
T_0	temperature at compressor inlet
s	entropy of bleed-air
s_0	entropy of air at compressor inlet

Enthalpy and entropy can be obtained from data tables when all the temperatures are known. The compressor inlet temperature is the total temperature (static + kinetic), while the compressor outlet temperature is the same as bleed temperature.

When the Auxiliary Power Unit (APU) is providing bleed-air, the bleed-air temperature is:

$$T_{bleed} = T_{total} \cdot 1.258 \tag{2.11}$$

, assuming that the pressure ratio is 2, and the compressor efficiency is 0.85. When the engines are running, the bleed temperature will be set by the engines and various conditions. Details about engine bleed and fan temperature are presented in chapter 6.

The shaft power for the conventional ACM is a sum of 3 different terms, shaft power for fresh air (bleed-air), shaft power for pre-cooler (bleed-air from engine fan) and shaft power for electric circulation fans:

$$P_{shaft,ACM} = P_{shaft,bleed} + P_{shaft,fan} + P_{shaft,cf} \tag{2.12}$$

With help from eq. 2.10 we can express these terms as:

$$P_{shaft,bleed} = \dot{m}_{air}[(h_{bleed} - h_{tot}) + T_{tot}(s_{bleed} - s_{tot})] \tag{2.13}$$

$$P_{shaft,fan} = \xi_{fan}\dot{m}_{air}[(h_{fan} - h_{tot}) + T_{tot}(s_{fan} - s_{tot})] \tag{2.14}$$

$$P_{shaft,cf} = \frac{P_{cf}}{\eta_{gbx} \cdot \eta_{gen} \cdot \eta_{trn} \cdot \eta_{mot}} \tag{2.15}$$

, where P_{cf} is the power for electric circulation fans, η_{gbx} is the gearbox efficiency, η_{gen} is the generator efficiency, η_{trn} is the transfer efficiency of electricity and η_{mot} is the motor efficiency.

2.3.2 Electric Air Cycle Machine Thermodynamics

The thermodynamic model for the conventional and Electric Air Cycle Machine (E-ACM) is the same, only difference is the source of compressed air and the shaft power calculation, since the power is taking a different path from the engine.

Beginning with the supply of compressed fresh air from the electrical compressor. The fresh air mass flow rate is the same as in previous case. The supply pressure is about 100 kPa above cabin pressure. The pressure ratio for the supply air is then:

$$\pi_{comp} = \frac{P_{cabin} + 100 \text{ kPa}}{P_{tot}} \tag{2.16}$$

Depending on flight condition and compressor efficiency, the compressed air temperature can be expressed as:

$$T_{comp} = T_{tot}\left[1 + \frac{\pi_{comp}^{\frac{\gamma-1}{\gamma}} - 1}{\eta_{comp}}\right] \tag{2.17}$$

, where π_{comp} is the pressure ratio, $\gamma = \frac{C_p}{C_v}$ is the ratio of specific heat for air. It changes with temperature but can be approximated to $\gamma \approx 1.4$ in this case. η_{comp} is the compressor efficiency.

Heat Exchangers

With the same precedure as with the conventional ACM, the cooling air mass flow rate through the heat exchangers is calculated as:

$$\xi_{hx} = \frac{\dot{m}_{hx}}{\dot{m}_{air}} = \frac{T_{comp} - T_{shx}}{(T_{comp} - \Delta T_{hx}) - T_{tot}} \tag{2.18}$$

Electric Air Cycle Machine Shaft Power

With help from eq. 2.10 , the compressor power can be calculated as:

$$P_{comp} = \dot{m}_{air}\left[(h_{comp} - h_{tot}) + T_{tot}(s_{comp} - s_{tot})\right] \tag{2.19}$$

This power comes from the engine shaft, through a gearbox, a generator, cables, power converters and a motor, all having an efficiency less than unity. Finally shaft power, that is extracted from the engine to the compressor and for the E-ACM, can be calculated:

$$P_{shaft,comp} = \frac{P_{comp}}{\eta_{gbx} \cdot \eta_{gen} \cdot \eta_{cpc} \cdot \eta_{mot}} \tag{2.20}$$

$$P_{shaft,EACM} = P_{shaft,comp} + P_{shaft,cf} \tag{2.21}$$

, where shaft power for the circulation fans, $P_{shaft,cf}$, is the same as in eq. 2.15.

2.3.3 Electric Vapour Cycle Machine Thermodynamics

Like the E-ACM, E-VCM also uses an electric air compressor to deliver air to the cabin, but at a lower pressure, since the pressurized air is not used to drive

the machine, as for the ACM. The air mass flow rate is set to a minimum, 6 g/paxs.

The supply pressure is about 20 kPa above cabin pressure. The pressure ratio for the supply air is then:

$$\pi_{comp} = \frac{P_{cabin} + 20 \text{ kPa}}{P_{tot}} \tag{2.22}$$

The compressed air temperature,T_{comp}, is calculated as in eq. 2.17.

VCM Operation

Since the fresh compressed air temperature is not as high as for the previous machines, cooling through heat exchangers is not always necessary. Often, heat exchangers must be throttled or even turned off. In extremely cold conditions, such as cruising at high altitudes, the electric heater is most likely to add additional heat to the cabin.

We begin with the supply air temperature for the cabin. When the speed is low and the solar heating effect must be considered, then the supply air temperature for the cabin can be expressed as:

$$T_{inlet} = T_{cabin} - \frac{U(A_{wet} - A_{prj})(T_{tot} - T_{cabin}) + U \cdot A_{prj}(T_{tot} + \Delta T_{solar} - T_c) + \dot{Q}_{pax}}{C_p \dot{m}_{air,min}} \tag{2.23}$$

When flying, the solar heating effect is neglected and we get:

$$T_{inlet} = T_{cabin} - \frac{U A_{wet}(T_{tot} - T_{cabin}) + \dot{Q}_{pax}}{C_p \dot{m}_{air,min}} \tag{2.24}$$

If cooling is needed by the Vapour Cycle Machine, then the cooling effect is expressed as:

$$\dot{Q}_{VCM} = \dot{m}_{air,min} C_p((T_{tot} + \Delta T_{hx}) - T_{inlet}) \tag{2.25}$$

The power to run the vapour cycle compressor is calculated as:

$$P_{comp,VCM} = \frac{\dot{Q}_{VCM}}{\text{COP}_\text{R}} \tag{2.26}$$

Coefficient of Performance Refrigerator (COP_R) can vary depending on temperatures and refrigerant but be set to 3, for simplicity. This means that 1 kW of power input to the VCM motor can pull out 3 kW of heat from the

system.

The cooling air mass flow rate through the primary and secondary heat exchangers are:

$$\dot{m}_{phx} = \dot{m}_{air,min} \frac{T_{comp} - (T_{tot} + \Delta T_{hx})}{(T_{comp} - \Delta T_{hx}) - T_{tot}} \tag{2.27}$$

$$\dot{m}_{shx} = \frac{\dot{Q}_{VCM}(1 + 1/COP_r)}{C_p(T_{shx} - T_{tot})} \tag{2.28}$$

If no cooling is required, then the vapour cycle compressor is turned off, $P_{comp,VCM} = 0$ and as a consequence, there is no cooling airflow through the secondary heat exchanger, $\dot{m}_{shx} = 0$.

Cooling air mass flow rate through the primary heat exchanger is throttled according to:

$$\dot{m}_{phx} = \dot{m}_{air,min} \frac{T_{comp} - T_{inlet}}{(T_{comp} - \Delta T_{hx}) - T_{tot}} \tag{2.29}$$

If heating is needed, then primary heat exchanger is turned off, $\dot{m}_{phx} = 0$, and the electric heater is turned on with a power of:

$$P_{eh} = -U \cdot A_{wet}(T_{tot} - T_{cabin}) - \dot{m}_{air,min} C_p (T_{comp} - T_{cabin}) - \dot{Q}_{pax} \tag{2.30}$$

Electric Vapour Cycle Machine Shaft Power

Power to compress supply air is expressed as:

$$P_{comp} = \dot{m}_{air,min} \cdot [(h_{comp} - h_{tot}) + T_{tot} \cdot (s_{comp} - s_{tot})] \tag{2.31}$$

The total shaft power to run the E-VCM is:

$$P_{shaft,EVCM} = \frac{P_{comp} + P_{comp,VCM} + P_{cf} + P_{hxf}}{\eta_{gbx} \cdot \eta_{gen} \cdot \eta_{trn} \cdot \eta_{mot}} + \frac{P_{eh}}{\eta_{gbx} \cdot \eta_{gen} \cdot \eta_{trn}} \tag{2.32}$$

,where power for the circulation fans ,P_{cf}, is the same as for the conventional ACM. Power to pull cooling air through the heat exchangers is P_{hxf}.

2.4 ECS Weight Impact

The weight of the ECS contributes to fuel consumption through Lift-to-Drag ratio of the aircraft. Increased weight leads to increased drag, while

drag transforms to fuel consumption by the engines' Thrust Specific Fuel Consumption (*TSFC*).

The mass of the ECS is a function of technology and rated power. Therefore Specific Power (*SP*) is chosen to distinguish different technologies. For the conventional ACM, bleed-air mass flow rate is chosen instead of power.

The specific power is used in the simulation to estimate ECS mass according to:

$$m_{ECS} = \frac{RP}{SP} \tag{2.33}$$

The rated power, *RP*, is a function of passenger count, pax, and data from several airliners with different sizes.

According to Tagge et al., 1985, [5], environmental control system modifications from the Baseline, 197 pax airliner with 2 engines, bleed-air ECS to a no-bleed electric ECS results in additional system mass, despite the removal of bleed associated ducting, valves and pre-coolers. See table 2.1. It is assumed that mass increase, associated with higher electric power demand by the ECS, also includes more powerful generators and transfer systems.

Table 2.1 – ECS mass and specific power for a 197 pax airliner. Amended from Tagge et al. 1985, [5]

Technology	Connected Power	Mass	Specific Power
Bleed ACM	2.00 kg/s	1034 kg	$1.93 \cdot 10^{-3}$ (kg/s)/kg
Electric ACM	262.5 kW	1533 kg	0.171 kW/kg
Electric VCM	202.8 kW	1633 kg	0.124 kW/kg

As described by Martinez, 2020, [10], we can read about the conventional ECS for the A320 (180 pax) and the A340 (400 pax). The A320 has 2 ACM packs and are rated for 2 kg/s of bleed-air. The A340 has 4 ACMs, while they are rated for 4 kg/s of bleed-air. The ECS for the A340 weighs 720 kg, which means 180 kg/pack. Martinez further describes that larger airliners usually have 1 pack per engine, each rated for 1 kg/s of bleed-air and weighs some 150 kg each. Note that mass presented here do not include the mass of bleed valves, pre-coolers and ducts. Thus we can not use these numbers for the ECS as a whole system.

Berlowitz, 2010, [6], described mass changes when fitting a couple of Wide-Body twin-engine airliners, about the same size as the A340, with electric instead of bleed ACM. See table 2.2. We can see that the removed

pneumatic parts, bleed-air valves, pre-coolers and ducts, weigh around 603 kg. For the A340 the packs mass is 720 kg, then the ECS mass is 720+603=1323 kg. If the rated bleed-air mass flow rate is 4 kg/s, then the mass-to-weight ratio is $4/1323 \approx 3.02 \cdot 10^{-3} \left[\frac{kg/s}{kg}\right]$. The power-to-weight ratio for the E-ACM can be estimated to 500kW/(1323+97)kg ≈ 0.352 kW/kg.

We can estimate approximately that the packs have the same mass as the pneumatic components. For the case with the A320, 2 packs weigh 300 kg, then the ECS mass would be around 600 kg. The bleed mass-to-weight ratio would then be $2/600 \approx 3.33 \cdot 10^{-3} \left[\frac{kg/s}{kg}\right]$.

Table 2.2 – ECS mass difference, comparing conventional Air Cycle Machine and the electric counterpart. The ECS is rated for 2x250 kW and is design for A330 and B767, around 400 pax. Amended from Berlowitz, 2010, [6]

Component	Mass difference [kg]
Generators 500 kW	150
Motors	150
Controllers	340
Compressors	60
Removed pneumatic parts	-603
Total	97

.

According to Chakraborty et al.,2016, [7], we can read that the electric architecture add weight to the aircraft, relative to the conventional architecture. See table 2.3. Assume that about 44%, $\frac{200\text{kW}}{540\text{kVA} \cdot 0.85} \approx 0.44$, of the rated power is used for the E-ACM.

Table 2.3 – Mass penalty by the Electric Air Cycle Machine for A320 sized airliner. Amended from Chakraborty et al.,2016, [7]

Component	Mass difference [kg]
Air compressors 200 kW	80
Generators 540 kVA	$0.44 \cdot (196 - 87) \approx 48$
Additional wiring	$0.44 \cdot 84 = 37$
Power electronics	$0.44 \cdot 130 = 57$
APU	$0.44 \cdot 98 = 43$
E-ACM weight penalty	265

As we saw previously that the conventional ECS for the A320 weighs about 600 kg. If we would convert to the E-ACM with associated electric

architecture, then there would be a mass penalty of 265 kg. The power-to-weight ratio for this E-ACM would then be $\frac{200\text{kW}}{600+265\text{kg}} \approx 0.231$ kW/kg.

According to Milewski, 2019, [11], there is a weight penalty when retrofitting an airliner with electric ECS, not to mention the re-certification time. For the A320, this weight penalty is estimated to be around 400 kg based on currently installed technology on the aircraft. Still, with more advanced technology can be reduced to 200 kg. If we compute the electric ECS power-to-weight ratio, we get $\frac{200\text{kW}}{600+200\text{kg}} = 0.250$ kW/kg.

To conclude the specific power of different ECS technology, we can see that the numbers, provided by Tagge et al., 1985, [5], deviates considerably from the rest. We can also see that the report was written 25-35 years ahead of the rest, so the values from that report will not be used directly, but as a reference to see the development of specific power.

For the other sources an average for the conventional Air Cycle Machine ECS mass-to-weight ratio is $3.18 \cdot 10^{-3} \left[\frac{kg/s}{kg}\right]$.

For the electric Air Cycle Machine ECS, the average system power-to-weight ratio is 0.278 kW/kg. Boeing B787 uses this system.

No modern studies could be found on the electric ECS with Vapour Cycle Machine. Still, if we assume the same leap in technology as with the electric Air Cycle Machine, then the power-to-weight ratio for the electric Vapour Cycle Machine ECS would probably be around 0.202 kW/kg.

A summary of ECS specific power for different technology is shown in table 2.4.

Table 2.4 – Summary of ECS specific power.

Technology	Specific Power
Bleed ACM	$3.18 \cdot 10^{-3}$ (kg/s)/kg
Electric ACM	0.278 kW/kg
Electric VCM	0.202 kW/kg

2.5 ECS Drag

While bleed-air results in shaft power loss, intake of air through scoops creates drag, which can be expressed with Newton's Second Law:

$$F = \frac{d(m \cdot v)}{dt} \tag{2.34}$$

Drag can directly be converted to fuel consumption by multiplying with *TSFC*.

The amount of mass flow rate of air through scoops, $\dot{m}_{scoops}$, is a sum of cooling air through the heat exchangers and intake of fresh air for the electric ECS. The air mass flow rate is determined by the ECS, while airspeed, v, is decided by the flight profile. We can formulate the drag as:

$$D_{scoops} = \dot{m}_{scoops} \cdot v \tag{2.35}$$

Effects of the shape of the air scoops and how they interact with the rest of the aircraft is believed to be small, thus have been neglected. Figure 2.5 shows the air scoops for the ECS packs. Their openings can be adjusted to regulate cooling of the heat exchangers in the ECS packs.

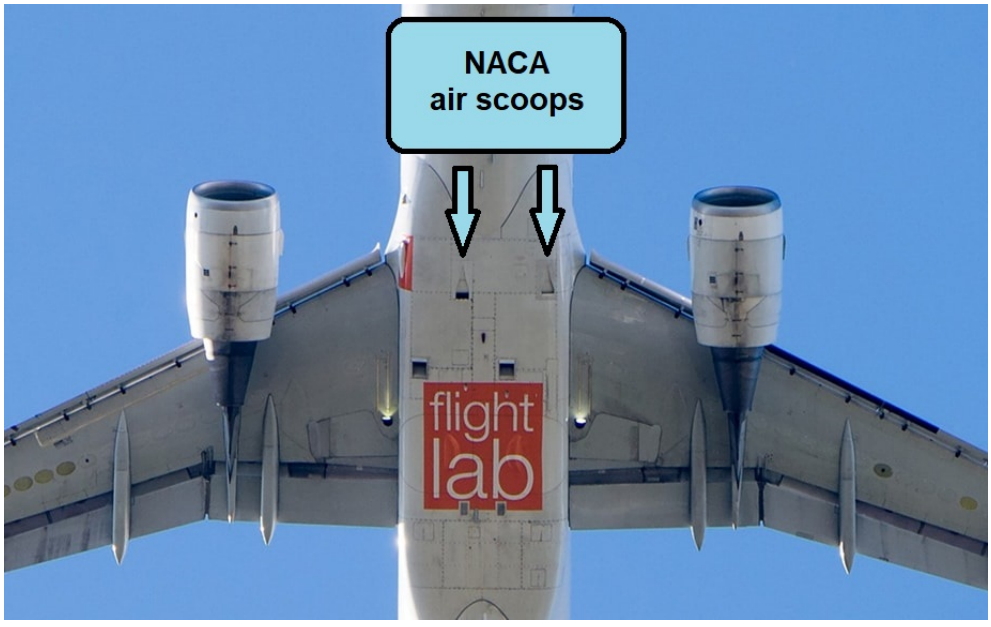

Figure 2.5 – Airbus A320 with partly open air scoops for the ECS. Amended from GKN Aerospace, [2].

2.6 ECS Fuel Consumption

Fuel consumption of the ECS is a function of shaft power for bleeding air, shaft power to run the machine, air intake induced drag, and lift induced drag. In some cases, the ECS can even force the engines to run at a higher thrust setting than what is needed by the aircraft, then the ECS should also be accounted for the thrust increased fuel consumption.

For the general ECS, fuel consumption can be formulated as:

$$\dot{m}_{fuel,ECS} = \dot{m}_{fuel,Pshaft} + \dot{m}_{fuel,drag} + \dot{m}_{fuel,mass} + \dot{m}_{fuel,thrust} \tag{2.36}$$

Fuel consumption due to shaft power to run the ECS is:

$$\dot{m}_{fuel,Pshaft} = kp \cdot TSFC \cdot P_{shaft,ECS} \tag{2.37}$$

Fuel consumption by the air scoop drag is:

$$\dot{m}_{fuel,drag} = TSFC \cdot D_{scoops} \tag{2.38}$$

Fuel consumption induced by mass of the ECS is:

$$\dot{m}_{fuel,mass} = TSFC \frac{m_{ECS} \cdot g}{LoD} \tag{2.39}$$

Fuel consumption for the ECS forced thrust increase is:

$$\dot{m}_{fuel,thrust} = TSFC \cdot \Delta T_{ECS} \tag{2.40}$$

kp is the Shaft Power Factor, g is the gravitational constant, *LoD* is the Lift-to-Drag ratio and ΔT_{ECS} is the ECS forced thrust increase.

Chapter 3

Aircraft Icing

Figure 3.1 – Ice on an aircraft wing, []

Before we delve deeper into ice protection, we need to understand why icing occurs and how it affects an aircraft. This chapter intends to answer the basics related to icing in aircraft.

3.1 Why and where does icing occur?

Following factors influence icing in aircraft:

1. **Supercooled Large Water Droplets (SLD)**: Aircraft undertakes flight through clouds consisting of supercooled droplets that contact the aircraft surface and freeze. The droplets accumulate over time to form an icing layer on the surface. The SLD is divided into two groups of MVD less than and greater than 40 μm [12].

2. **Precipitation**: Water droplets from rain or snow freeze on contact with the aircraft surface. When the air temperature lies between 0 C and 3 C , the snow consists of liquid water. This liquid water, in turn, causes the snow crystals to form weak bonds with each other. The weak bonds turn into strong bonds when the air temperature falls below 0 C (Dalili et al, 2009) [13] [14].

There have been numerous experiments to ascertain the effects of icing in aircraft. We observe that icing affects the aircraft's primary aerodynamic forces, i.e., lift, weight, thrust, and drag. The observable parameters that support this finding are the drag, lift coefficients, and the mass of ice produced. As a consequence, icing poses a significant threat that causes effects such as loss in altitude, airspeed, and lift while at the same time increasing power consumption of other aircraft subsystems.The locations of icing occurrence include leading edges of airfoil, tailgate, cockpit glass, windows, pitot tube, antennas and inlet tip of engine nacelles.

3.2 Ice Types

1. **Rime Ice** : Rime ice is created when SLD hit the surface of aircraft, and quickly freeze on impact. It has a milky-white and crystalline appearance. The favorable conditions for rime ice include small, supercooled droplets present in stratiform clouds. Airfoil shape and leading edges near the engine inlet are the locations where there is a possibility of rime ice formation. It is formed where there is zero local velocity of the fluid (stagnation point) [15].

2. **Glaze/Clear Ice** : It is a thick layer of glass-like ice created while the aircraft is in flight where there is a high availability of SLD. A small part of the droplet hits the surface of the aircraft, and gradually freezes

on impact. In some cases, there is uneven distribution of glaze ice throughout the wing surface, as observed from Figure XX.The favorable conditions for glaze ice include large droplets present in cumuliform clouds, freezing rain or terrain effects.

Insert weather.gov reference zhu training page, and insert figure number

3. **Mixed Ice**: Mixed ice has both Rime and Glaze ice properties. It has a rugged and opaque appearance. The favorable conditions for mixed ice include the coexistence of large and small droplets, liquid and frozen particles, and wet snow.

Reference : NACA 23015 generated from XFoil modified to show Ice Types

3.3 Cloud Types

The scope of the study covers Continuous Maximum (CM) Stratiform and Intermittent Maximum (IM) for Cumuliform Clouds.

1. **Cumuliform Clouds** : Formed due to severe convection, they are heavy and can hold a high LWC. The constrained horizontal extent is exposed to the aircraft for a short period.

2. **Stratus Clouds**: Formed due to less severe convection than Cumuliform Clouds.The stratified layer thus formed covers a wide area. They are not as heavy, however can sometimes hold a high LWC. Also called as layer clouds. Icing layers are uncommon with a vertical extent of more than 3.000 ft.

3. **Freezing Rain** : Significant icing happens while the aircraft is flying on cold air mass and below a warm air layer. Raindrops have a larger capture rate than cloud droplets. They form clear ice at freezing temperatures.

4. **Freezing Drizzle** : Drizzle falls from stratus clouds which have a high LWC.

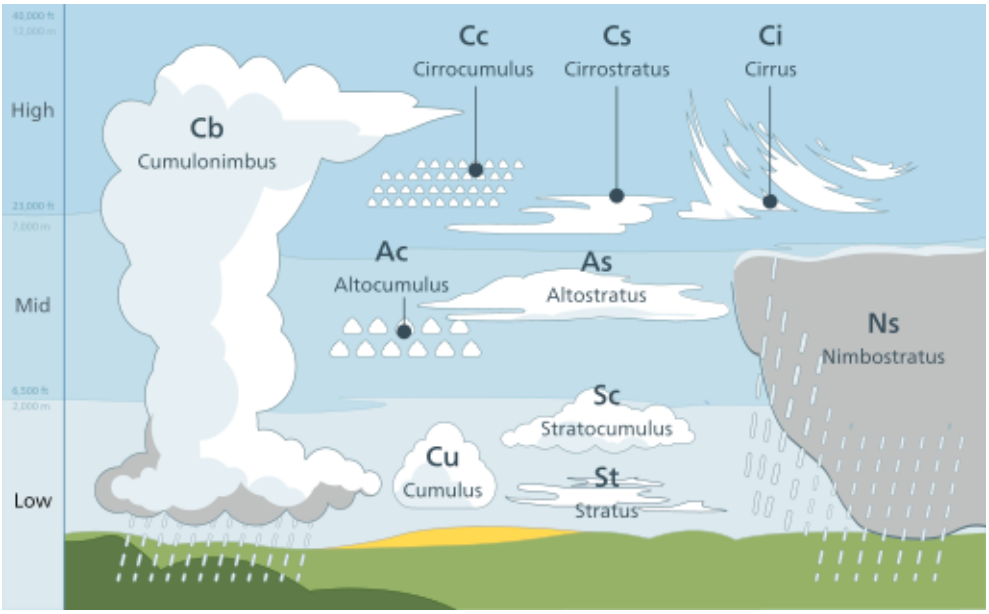

Figure 3.2 – Cloud Types [3]

3.4 Parameters for Icing formation

Average droplet size, liquid water content, and the air temperature primarily constitute the deterministic parameters for the icing conditions.

3.4.1 Drop Median Volumetric Diameter (MVD)

Testing acronyms: Median Volumetric Diameter, which is abbreviated MVD.

Drop median volumetric or otherwise called as median droplet diameter, refers to the center point droplet size, where half of the amount of the droplet is smaller, and the other half of the droplets is larger than the mean droplet volume. The extent of the aft limit of the IPS is usually calculated with a 40 micron MVD , as prescribed by FAA. MVD of 40 microns reveals that half of the volume is less than 40 microns of droplet size, while the other half is more than 40 microns.

reference Aircraft icing handbook

3.4.2 Droplet Distribution

It is necessary to know the droplets' size to explain and predict icing simulations accurately. Langmuir and Blodgett (1946) proposed a monodisperse droplet distribution in which half of the droplets had a smaller radius and the other half a larger radius in the fog. Monodispersion is a commonly used method and has been chosen as one of the input icing design parameters. Additionally, Langmuir D distribution is selected for the icing simulations. The Langmuir D distribution contains a set of seven ratios of diameters corresponding to the percentage of LWC. For a given MVD, there are seven values in a Langmuir D distribution. In the past, NACA has used distributions published by Langmuir to assess MVD that are now in Appendix C. The upper limit for Langmuir-D distribution is an MVD of 50 microns. Figure 3.3 depicts the 7-diameter Langmuir-D distributions separately. The dashed line represents the final solution generated using weights on each droplet size.

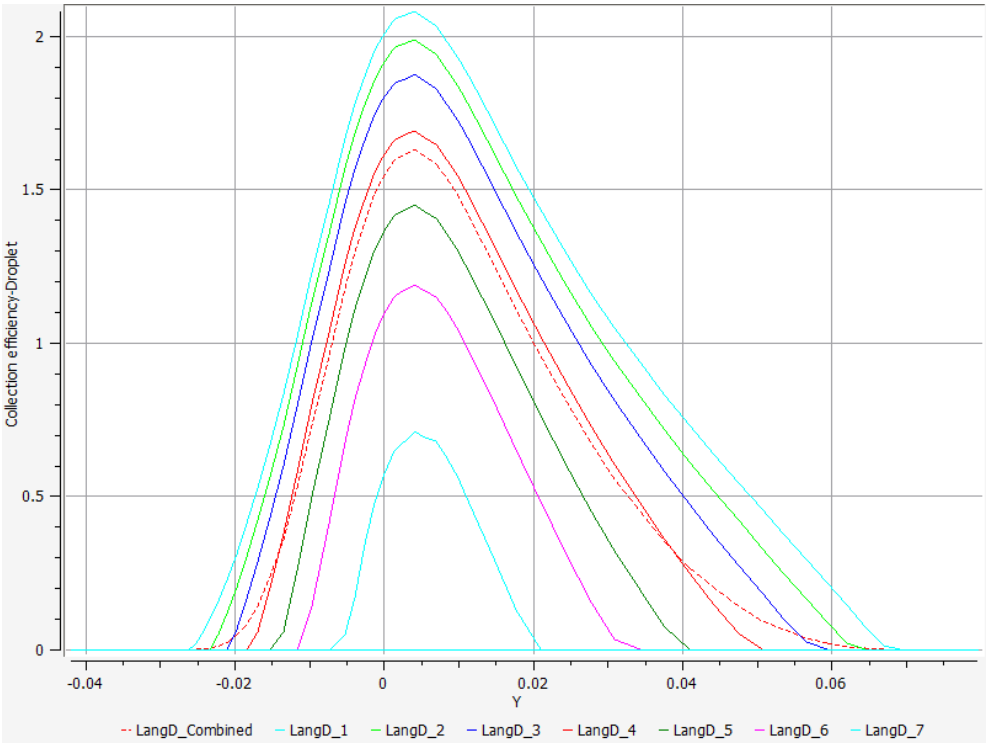

Figure 3.3 – Langmuir D Distribution for Climb Case Study as computed by FENSAP-ICE [3]

Reference for FENSAP-ICE

3.4.3 Droplet Impingement

In order to evaluate the thermal inputs for removing ice accumulation, the design of ice protection systems includes awareness of local and total impingement intensities. Experiments have been performed in the past by NASA Glenn Research Center and at the FAA Technical Center. In a typical experiment setup, the data is captured through a Charge Coupled Device Camera. These devices specialize in capturing highly sensitive optical signals. Analysis is typically performed on components such as Finite Wings, Inlets of engines and Airfoils, The droplet distribution is around a MVD of 16,5 and 20,4 microns. Droplet impingement is mathematically characterized by the Collection efficiency. The collection efficiency is the fraction of liquid water in the path of an aircraft component that, when traveling in icing conditions, is accumulated as ice on that component.

Reference Skybrary icing collection efficiency

3.4.4 Liquid Water Content (LWC)

The LWC is a parameter which influences the rate of ice accretion, the icing type, and risk of runback water freezing behind the protected areas.

Reference Comparison of LWC NASA apps.dtic.mil

It is the *liquid water quantity per unit volume of air*. It is calculated from Appendix C, corresponding to MVD, ambient temperature and pressure altitude for a standard horizontal extent. It is measured in g/m^3. The higher the LWC, the higher the amount of ice accretion.

Reference Petra thorsson

3.4.5 Icing Air Temperature (Ambient Temperature)

Icing Air temperature is the subzero Celsius temperature corresponding to ice formation. It is measured in C.

3.4.6 Horizontal Extent

The horizonal extent is defined as the extent or height of air mass corresponding to the cloud. It is measured in nm.

3.4.7 Vertical Extent

The vertical extent is defined as the extent or depth of air mass corresponding to the cloud. It is measured in nm.

3.5 Icing Standards

The IPS must certify airworthiness requirements for flights into icing conditions. At present, the safety regulation is pursuant to Appendix C, Amendment 24, CS-25 of European Union Safety Agency (EASA) *ED Decision 2020/001/R*. The primary objective of Appendix C is to provide the highest possible (99%) icing conditions that the IPS should endure . According to Appendix C Part 1, for a non standard horizontal extent, the LWC is calculated by multiplying the LWC values of standard horizontal extent, by the liquid water content factor F corresponding to the non-standard horizontal extent. Appendix O provides the data for calculating the LWC for a non-standard horizontal extent subject to freezing rain and freezing drizzle conditions.

Subsequently, Appendix O provides SLD, freezing drizzle and freezing rain icing conditions pursuant to Amendment 24, CS-25 of European Union Safety Agency (EASA) *ED Decision 2020/001/R*.

Reference for CS 25.

3.5.1 Design Standards

Based on the Appendix C, we have the following parameters for continuous maximum or Stratiform clouds:

1. Cloud LWC should be between 0.14 g/m^3 and 0.18 g/m^3 (for $0C$).
2. The ambient or aircraft surface temperature should be below $0C$.
3. The air temperature should be above -30C.
4. Maximum vertical extent of 2000 m (6.500 ft).
5. Horizontal extent has a standard value of 17.4 nautical miles, or 32.2 km.
6. Pressure altitude ranges from sea level to 6.700 m (22.000 ft).
7. The MVD should lie in the range between 15 microns and 40 microns.

Based on the Appendix C, we have the following parameters for intermittent maximum or Cumuliform clouds:

1. Cloud LWC should be between 0.14 g/m^3 and 2.76 g/m^3 (for 0C).
2. The ambient or aircraft surface temperature should be below 0C.
3. The air temperature should be above -40C.
4. Maximum vertical extent of 2000 m (6.500 ft).
5. Horizontal extent has a standard value of 2.6 nautical miles, or 4.94 km.
6. Pressure altitude ranges from 1200m (4.000 ft) to 6.700 m (22.000 ft).
7. The MVD should lie in the range between 15 microns and 50 microns.

Chapter 4

Ice Protection System

This chapter a comprehensive overview of the Ice Protection System (IPS) and its types. Additionally, it describes the factors that influence IPS power consumption.

4.0.1 Mechanism of Ice Protection

In certain situations, snow and ice protection can also be provided to the aircraft when it is not in flight (or grounded) by spraying Type 1 Fluid diluted with water. The Type I fluid consists of propylene glycol, which is heated to a termperature of 60 to 65 Degrees Celsius. The system that operates to remove ice buildup is called a de-icing system. In contrast, the system used to avoid ice buildup is called an anti-icing system. For the anti-icing system, the fluid used is Type IV, which is a more viscous version of Type I, not mixed with water. Propylene glycol is non-toxic, whereas Ethylene glycol, another lesser-known substance used, is toxic. The pilots disable the aircraft's ventilation system to prevent fluid fumes from entering inside during the application of Type I and Type IV Fluids. *Type IV fluids gradually lose effectiveness during flight, and this is where the standard electrothermal and pneumatic ice protection systems come into play.*

https://thepointsguy.com/news/how-aircraft-de-icing-works

4.1 IPS Function

The function of the IPS is to provide ice protection to various crucial components that come in *direct contact* with ice, be it during flight or when the aircraft is

on the ground. For MEA technologies, the need to incorporate the IPS arises from the fact that IPS plays a significant role in electrical power consumption.()
add reference here for previous studies

4.2 IPS Types

4.2.1 Wing Ice Protection System (WIPS)

WIPS focuses on the ice protection of the leading edges of the aircraft wings. Pneumatic Evaporative Anti-icing system Electrothermal Running-wet anti icing WIPS ‘

Pneumatic Evaporative Anti-icing system WIPS

Electrothermal Running-wet anti icing WIPS

The performance of bleed-air or electro-thermal ice protection systems (IPS) can be studied with FENSAP-ICE through the conjugate heat transfer (CHT) between air, water, ice and the solid materials that compose the IPS. The airflow domains are separated from the metal or composite skin of the aircraft component;, therefore, all the ANSYS airflow solvers can be used. For bleed-air systems, a steady-state thermal equilibrium between domains is computed to verify that the protected region is free of ice. For electro-thermal systems, the IPS response time to the cyclic activation of heater pads is analyzed in a time-dependent CHT simulation encompassing phase change, heat conduction and water runback to accurately predict the amount of ice that forms, melts and refreezes. A wide variety of IPS configurations can be analyzed.

4.2.2 Cowl Ice Protection System (CIPS)

4.3 IPS Thermodynamics

reference developments.docx

4.3.1 Pneumatic Evaporative Anti-icing system WIPS

4.3.2 Electrothermal Running-wet anti icing WIPS

Extent of Protection (EOP)

4.4 IPS Weight Impact

4.5 IPS Drag

Since we have chosen the de-icing designs, there are no drag-penalties involved.

Chapter 5

IPS Research Methodology

5.0.1 Model Selection

- Spalart-Allmaras Turbulence Model
- K-omega SST Model
- K-Epsilon Model
- Rationale for model selection(limitations,advantages)

5.0.2 Software Package Selection

- Available Alternatives

Rationale for software selection openness,limitations,advantages,latest

Importance has been given to the fact that students and researchers should repeat the conditions described in this study to get the same results. The ANSYS SpaceClaim and ANSYS FENSAP-ICE software package available is bleeding-edge. However, both help us to attain the objective within respectable assumptions. Additionally, ANSYS FENSAP-ICE is the only software that has an extensive set of features necessary for IPS.

5.0.3 Input Parameter Selection

According to the flight profile, two parameters are selected, namely Climb and Descent. The values for the parameters are illustrated in Tables 5.1 and 5.2. For both of the cases, the air pressure at specified altitude is calculated

Temperature at Sea Level (K)	288,15	
Pressure at Sea Level (Pa)	101325	
Altitude (ft)	6000	
Altitude (m)	1828,8	
Air static pressure at altitude (Pa)	78919,78	
Droplet Diameter	20	
Droplet Distribution	Langmuir D	
Air Velocity (m/s)	80	
Aircraft Speed (m/s)	190,25	
Icing air Temperature (K)	256	
Icing Duration (seconds)	500	
Clouds	Continuous Maximum or Stratiform	Intermittent Maximum or Cumuliform
Ice Type	Rime	Glaze Advanced

Table 5.1 – Input Climb Parameters

from the barometric atmospheric relation between pressure and temperature at sea level. The altitude is selected to be $6000ft$ as in this altitude; there is a possibility of forming both stratus and cumulus clouds. A standard NASA-grain surface roughness of

enter value

is used. INSERT Barmetric formula

Climb Input Parameters

During Climb, there is a lot of power utilized to overcome drag and produce lift. When it comes to icing, the average speed taken from the flight log for our case study comes out to be 190,25 m/s. Icing is assumed to happen over a total duration of 500 seconds (or 8.33333 minutes). Consulting Appendix C Stratiform for droplet MVD 20 µm subject to specified air temperature and altitude, the LWC is calculated. The LWC is corrected for total accumulation time and cloud type to improve on the solution by introducing a correction factor. The new LWC value is then used as input for the droplet simulation. Similarly, consulting Appendix C Cumuliform for droplet MVD 20 microns, the LWC is calculated to be 0,255 g/m^3.

Descent Input Parameters

During Descent, there is a lot of drag induced because of application of flaps and brakes. When it comes to icing, the average speed chosen from the flight log for our case study comes out to be 202,75 m/s.

Langmuir D Distribution

Insert table Langmuir D Distribution of droplets with MVD 20 μm$usedfortheestudy$.

Temperature at Sea Level (K)	288,15	
Pressure at Sea Level (Pa)	101325	
Altitude (ft)	6000	
Altitude (m)	1828,8	
Air static pressure at altitude (Pa)	78919,78	
Droplet Diameter	20	
Droplet Distribution	Langmuir D	
Air Velocity (m/s)	80	
Aircraft Speed (m/s)	202,75	
Icing air Temperature (K)	256	
Icing Duration (seconds)	500	
Clouds	Continuous Maximum or Stratiform	Intermittent Maximum or Cumuliform
Ice Type	Rime	Glaze Advanced

Table 5.2 – Input Descent Parameters

Real-Life Parameters Stockholm Copanhagen flight

Standard NASA Parameters

Consult page 2-F 201 of CS 25 for IPS wind tunnel testing parameters

LWC is output parameter. create a flow diagram explaining the unput and putput parameters.

5.0.4 Simulation

Geometry

XFoil

Meshing

Gmsh,ANSYS Meshing Very time consuming since orrthogonal quality is difficult to achieve in 3D meshing.A compromise between 1.5 million mesh elements and defeaturing is the objective.

Automation

IronPython scripting (Enclosure and Surface Automation), ANSYS Workbench Journal Scripting

Mesh Optimization

Mesh size, orthogonal quality, y+ value, OPTIGRID

Icing simulation

Discussion of FENSAP-ICE, DROP3D, ICE3D, CHT3D Pneumatic, CHT3D Electrothermal.

The physics and in-flight icing thermodynamics consist of strong heat convection in fluids. Realistic simulations of IPS are too complex to be treated within a single computational domain. The computationally efficient alternative is to apply a divide and conquer strategy by computing the solutions of the different domains separately and exchanging interface boundary conditions in an iterative manner. Convergence is achieved by equalizing heat fluxes and temperatures across interfaces. The strategy also benefits from simplification of mesh modeling.

Chapter 6

Bleed Temperature

Short description why bleed temperature is important.

6.1 CFM International CFM56-5B

Describe the CFM56-5B roughly. Show bleed ports.

6.1.1 Engine Maps

Engine maps. Show how bleed temperature is a function of thrust.

Include picture.

6.2 Síde note on Pneumatic WIPS

Engine maps. Why icing is dependent to bleed temperature.

Chapter 7

Flight dynamics

Describe why flight dynamics is important, how it affect fuel consumption.

7.1 Flight profile

Describe flight profile, where it comes from and how it is used.

7.2 Takeoff mass

What is takeoff mass and how it is derived?

7.2.1 Zero-fuel mass

What is zero-fuel mass and how it is derived?

7.2.2 Fuel mass

Show how to estimate fuel mass?

7.3 Lift

Show how lift is a function of mass and flight profile.

7.4 Drag

What is drag and all its components?

Explain how drag affect fuel consumption and bleed temperature?

7.4.1 Zero-lift drag coefficient, CD_0

Show the component build-up method.

7.4.2 Lift-induced drag coefficient, k

Data from OpenAP.

7.4.3 Flaps effect on drag

7.4.4 Effect of landing gear on drag

7.4.5 Wave drag

7.4.6 Sum of all drag

7.5 Thrust

How is the required thrust calculated?

Chapter 8

Thrust Specific Fuel Consumption (TSFC)

Show how TSFC was derived.

Show propulsive fuel consumption as function of thrust.

Chapter 9

Shaft power to fuel consumption

Show how all kinds of secondary power can be converted to shaft power.

Show how shaft power can be converted to fuel consumption.

Chapter 10

Miscellaneous loads

Show all other loads, described by previous work.

10.1 Airliner Subsystems

Describe a typical airliner with most subsystems. The energy flow from the engines to the subsystems. Differences with MEA.

Include pictures.

10.2 Load comparison

Compare all kinds of loads (fuel consumption with pie charts), to see how they relates to one another.

Chapter 11

Compare conventional aircraft and MEA

Compare fuel economy in 3 different units: kg fuel per seat km, litre fuel per seat km, seat km per litre.

Explain differences.

Pros and cons. Also those that are not related to fuel economy.

Include graphs.

Mass of Ice in kg

Chapter 12

Pax-scaling effect on fuel economy

Show how pax-scaling is affecting fuel economy.

Size matter, but not in the expected way. Explain why.

Include graphs.

Chapter 13

Results and Objective Analysis

svensk: Resultat och Analys

Sometimes this is split into two chapters. Keep in mind: How you are going to evaluate what you have done? What are your metrics? Analysis of your data and proposed solution. Does this meet the goals which you had when you started?

Power consumption for IPS

Other Results from FENSAP Simulation

In this chapter, we present the results and discuss them.

I detta kapitel presenterar vi resultatet och diskutera dem.

Ibland delas detta upp i två kapitel.
Hur du ska utvärdera vad du har gjort? Vad är din statistik?
Analys av data och föreslagen lösning
Innebär detta att uppnå de mål som du hade när du började?

13.1 ECS Fuel consumption

A case study was done with the Airbus A320 and 180 pax on a round trip Copenhagen-Stockholm-Copenhagen on a hot day. Figure 13.1 shows a breakdown of the fuel consumption of all 3 ECS configurations. We can see that the ACM and E-ACM are fairly equal in operational efficiency. If we add the effect of weight and drag, then the E-ACM becomes an inferior option. However, in this particular case, for the bleed-air driven ACM, there

were some moments when the ECS forced the engines to run at a higher thrust setting than was required by the aircraft. This happened at high altitude during descent. The combination of low ambient pressure, at high altitude, and low thrust setting, resulted in too low bleed pressure from the engines. To maintain normal operation of the ACM, the ECS then forced the engines to run at a higher power setting. If we take this thrust increased fuel consumption into consideration, then the conventional ACM has a clear disadvantage over the electrical options.

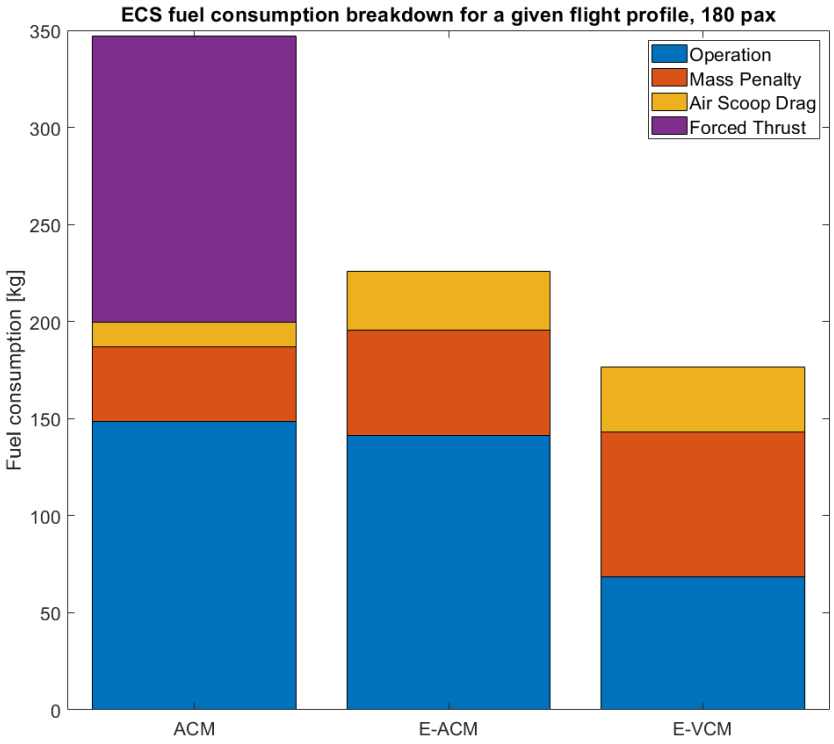

Figure 13.1 – ECS fuel consumption breakdown for a round trip flight, Copenhagen-Stockholm-Copenhagen, with a modelled A320 and 180 pax.

The VCM has the most efficient operation, consuming about half the amount of fuel than the ACM. But the weight penalty and increased drag offsets the operational efficiency, almost entirely.

13.2 ECS Partial Results

This section will show and discuss important partial results from a simulation of the case study. Three different airliners were simulated in parallel. They are all based on the same A320 sized aircraft with 180 pax, but with different ECS, flying on the same path. The flights took place between Copenhagen and Stockholm, back and forth. A hot day (30 °C on the ground) was chosen because the heat will stress the ECS to work harder, which will probably magnify the systems' differences.

We begin with the Air Mass Flow Rates. Figure 13.2 shows air mass flow rates for all 3 systems.

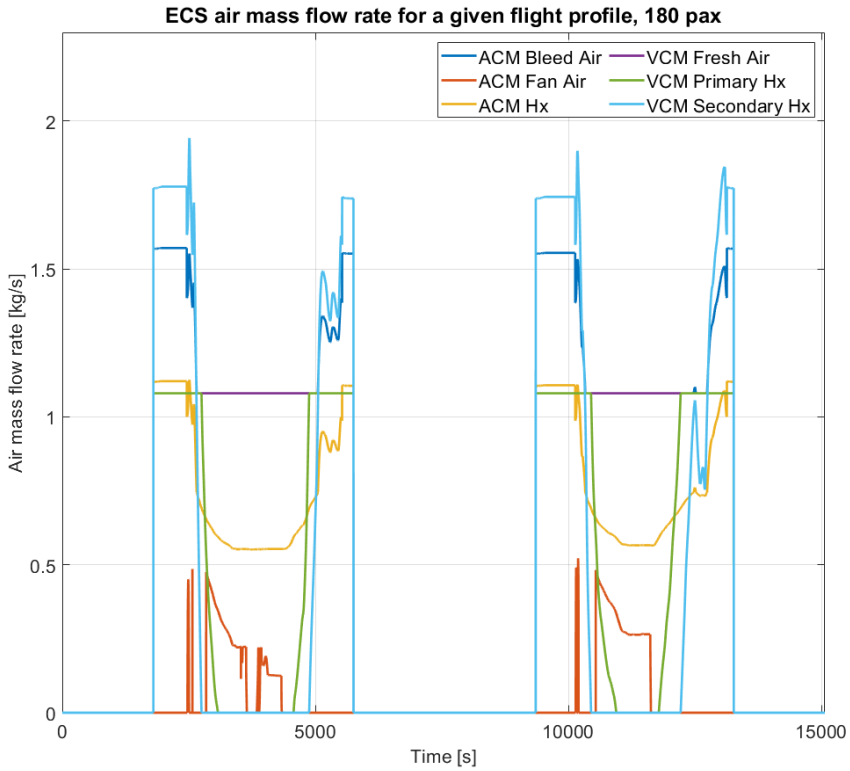

Figure 13.2 – ECS air mass flow rates.

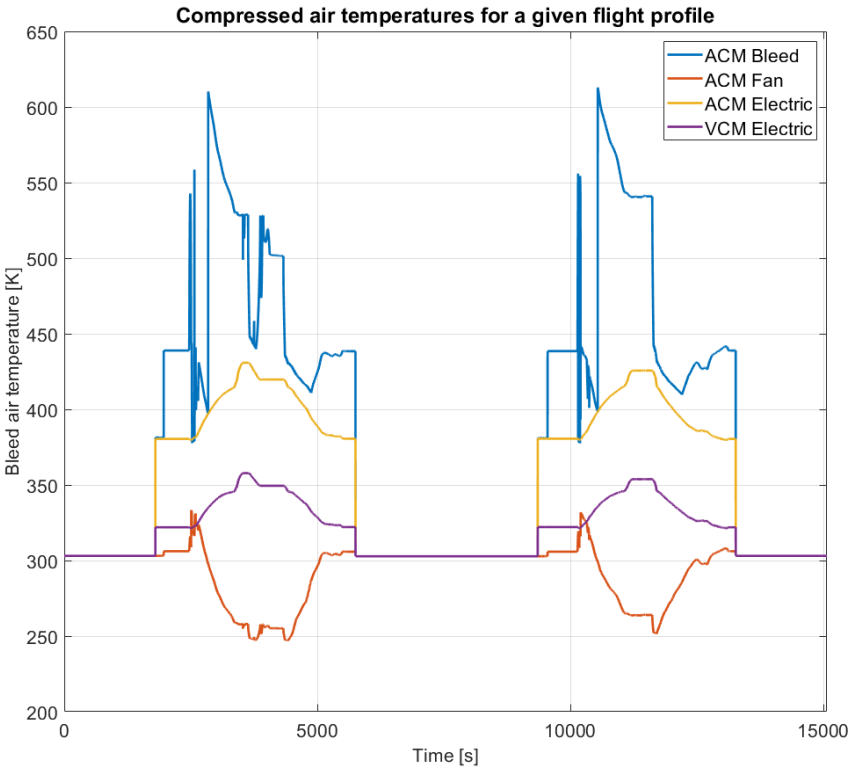

Figure 13.3 – Compressed air temperatures.

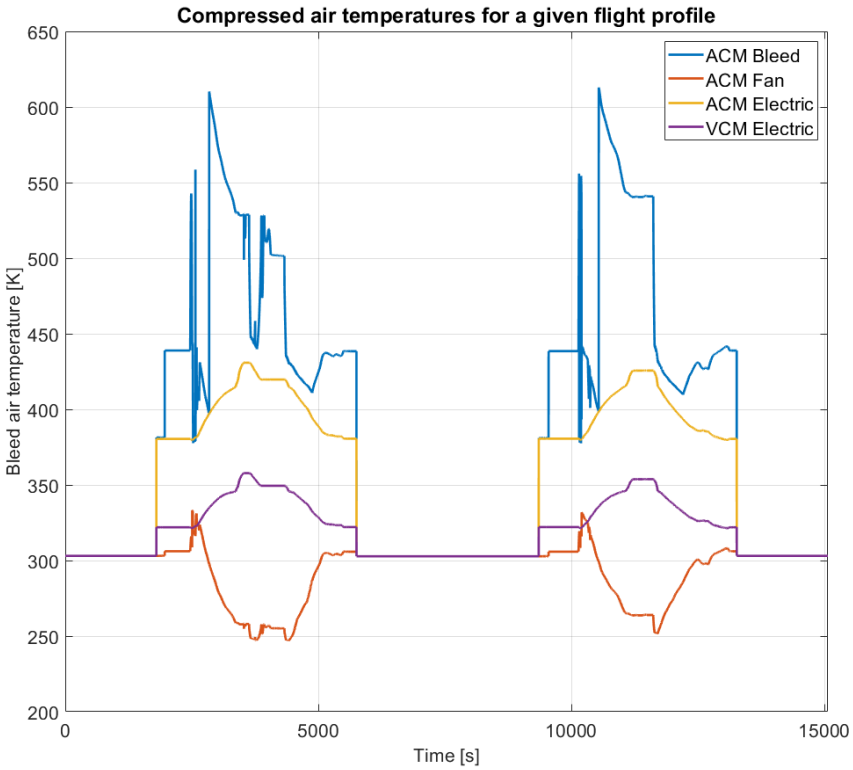

Figure 13.4 – Compressed air temperatures.

13.3 Reliability Analysis

Analys av reabilitet

Reabilitet i metod och data

13.4 Validity Analysis

Analys av validitet

Validitet i metod och data

Chapter 14

Discussion(Subjective Analysis)

This can be a separate chapter or a section in the previous chapter.

Diskussion

Förbättringsförslag?

Appendix C and SLD do not work together!

Chapter 15

Conclusions and Future work

Slutsats och framtida arbete

Add text to introduce the subsections of this chapter.

15.1 Conclusions

Describe the conclusions (reflect on the whole introduction given in Chapter 1).

Slutsatser

Discuss the positive effects and the drawbacks.
Describe the evaluation of the results of the degree project.
Did you meet your goals?
What insights have you gained?
What suggestions can you give to others working in this area?
If you had it to do again, what would you have done differently?

Träffade du dina mål? Vilka insikter har du fått? Vilka förslag kan du ge till andra som arbetar inom detta område? Om du hade att göra igen, vad skulle du ha gjort annorlunda?

15.2 Limitations

What did you find that limited your efforts? What are the limitations of your results?

1. Empenage not considered
2. Only steady state conditions are considered.
3. COWL Ice Protection system (CIPS) not implemented for simulations.

User defined distributions are not yet supported.

Begränsande faktorer

Vad gjorde du som begränsade dina ansträngningar? Vilka är begränsningarna i dina resultat?
För IPS

1. Empennage inte beaktas.
2. Endast stabila tillstånd beaktas.
3. COWL Ice Protection System (CIPS) inte implementerat för simuleringar.

15.3 Future work

Describe valid future work that you or someone else could or should do. Consider: What you have left undone? What are the next obvious things to be done? What hints can you give to the next person who is going to follow up on your work?

Vad du har kvar ogjort?
Vad är nästa självklara saker som ska göras?
Vad tips kan du ge till nästa person som kommer att följa upp på ditt arbete?

COWL Ice Protection

Due to the breadth of the problem, only some of the initial goals have been met. In these section we will focus on some of the remaining issues that should be addressed in future work. ...

simulink model

15.3.1 What has been left undone?

15.3.2 Next obvious things to be done

In particular, the author of this thesis wishes to point out xxxxxx remains as a problem to be solved. Solving this problem is the next thing that should be done. ...

15.4 Reflections

What are the relevant economic, social, environmental, and ethical aspects of your work?

Reflektioner

Vilka är de relevanta ekonomiska, sociala, miljömässiga och etiska aspekter av ditt arbete?

In the references, let Zotero or other tool fill this in for you. I suggest an extended version of the IEEE style, to include URLs, DOIs, ISBNs, etc., to make it easier for your reader to find them. This will make life easier for your opponents and examiner.
IEEE Editorial Style Manual: `https://www.ieee.org/content/dam/ieee-org/ieee/web/org/conferences/style_references_manual.pdf`

Låt Zotero eller annat verktyg fylla i det här för dig. Jag föreslår en utökad version av IEEE stil - att inkludera webbadresser, DOI, ISBN etc. - för att göra det lättare för läsaren att hitta dem. Detta kommer att göra livet lättare för dina motståndare och examinator.

References

[1] J. A. Parrilla, "Hybrid environmental control system integrated modeling trade study analysis for commercial aviation," *SAE Technical Papers*, vol. 2014-September, no. September, 2014. doi: 10.4271/2014-01-2155

[2] *Additive Manufacturing - AM enables industry-first for Airbus*, Accessed January 26, 2021. [Online]. Available: https://www.gknaerospace.com/en/our-technology/2017/am-enables-industry-first-for-airbus/

[3] W. G. Habashi, M. Aubé, G. Baruzzi, F. Morency, P. Tran, and J. C. Narramore, "Fensap-Ice : a Fully-3D in-Flight Icing Simulation System for Aircraft , Rotorcraft and Uavs," *24th International Congress of the Aeronautical Sciences*, pp. 1–10, 2004. [Online]. Available: http://www.icas.org/ICAS_ARCHIVE/ICAS2004/PAPERS/608.PDF

[4] E. H. Hunt, D. H. Reid, D. R. Space, and F. E. Tilton, "Commercial Airliner Environmental Control System: Engineering Aspects of Cabin Air Quality," *Aerospace Medical Association annual meeting*, pp. 1–8, 1995. [Online]. Available: https://web.archive.org/web/20120331055732/http://www.cabinfiles.com/?CFrequest=file;03032001100119

[5] G. E. Tagge, L. A. Irish, and A. R. Bailey, "Systems Study for an Integrated Digital/Electric Aircraft (IDEA)," *NASA Contractor Report 3840, NASA-CR-3840 19850007405*, 1985.

[6] I. Berlowitz, "All / More Electric Aircraft Engine & Airframe Systems Implementation," *The 9th Israeli Symposium on Jet Engines and Gas Turbines (Oct 7, 2010)*, pp. 1–48, 2010.

[7] I. Chakraborty, D. N. Mavris, M. Emeneth, and A. Schneegans, "An integrated approach to vehicle and subsystem sizing and analysis for novel subsystem architectures," *Proceedings of the Institution of*

Mechanical Engineers, Part G: Journal of Aerospace Engineering, vol. 230, no. 3, pp. 496–514, 2016. doi: 10.1177/0954410015594399

[8] M. Merzvinskas, C. Bringhenti, J. T. Tomita, and C. R. De Andrade, "Air conditioning systems for aeronautical applications: A review," *Aeronautical Journal*, vol. 124, no. 1274, pp. 499–532, 2020. doi: 10.1017/aer.2019.159

[9] R. Slingerland and S. Zandstra, "Bleed air versus electric power off-takes from a turbofan gas turbine over the flight cycle," *Collection of Technical Papers - 7th AIAA Aviation Technology, Integration, and Operations Conference*, vol. 2, no. September, pp. 1516–1527, 2007. doi: 10.2514/6.2007-7848

[10] I. Martinez, "Aicraft Environmental Control System," pp. 1–31, 2020.

[11] D.M.N. Milewski, "Effect of Electric Environmental Control System Retrofit on Fuel Burn of a Medium-Range Aircraft," p. 104, 2019. [Online]. Available: http://resolver.tudelft.nl/uuid:198055ea-d3b2-41b4-897e-9fb43f514265

[12] European Aviation Safety Agency, "Certification Specifications and Acceptable Means of Compliance for Large Aeroplanes CS-25 : Amandment 24," European Union Aviation Safety Agency, Tech. Rep. Amendment 17, jan 2020.

[13] P. Thorsson, "Modelling of Atmospheric Icing," Tech. Rep.

[14] N. Dalili, A. Edrisy, and R. Carriveau, "A review of surface engineering issues critical to wind turbine performance," Tech. Rep. 2, feb 2009.

[15] "Icing Conditions - CAV Systems." [Online]. Available: https://en.wikipedia.org/wiki/Icing_conditionshttps://www.cav-systems.com/icing-conditions/

Appendix A

Extra material

Show all input parameters?

Show the MATLAB code?

svensk: Extra Material som Bilaga

A.1 Miscellaneous Data

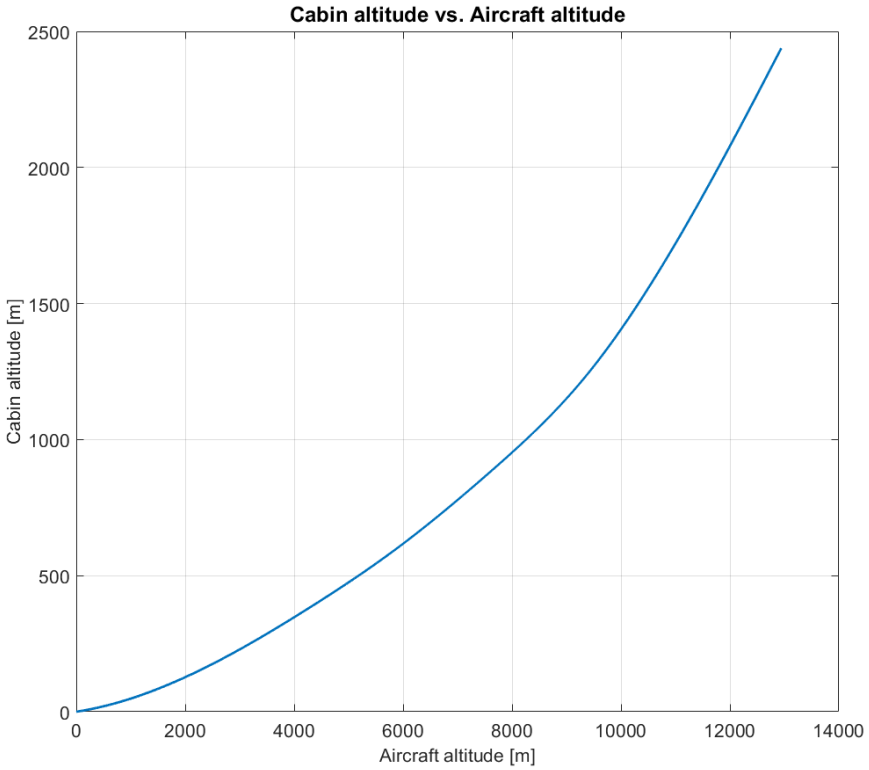

Figure A.1 – Cabin altitude. Amended from Hunt et al., 1995, [4]

A.2 MATLAB Code

Listing A.1 is showing a code example in MATLAB format.

Listing A.1 – Fuel calculations.

```
% Testing to include MATLAB code in LaTeX
% ####### VCM ECS fuel consumption #######
if mode == 1
    % Power from APU, 2 kg/min for 447 kW (Honeywell 131-9A), Dieter Scholz
    % - An Optiomal APU for Passenger Aircraft, 2015
    E_VCM_Fuel = 7.4571e-8 * shaftpower_VCM_ecs; % [kg/s] Fuel consumption
    % of ECS and circulation fans
elseif mode==2 || mode==9 % Power from main engines on ground
    % [kg/s] Fuel consumption of ECS and circulation fans
    E_VCM_Fuel = kp*tsfc*shaftpower_VCM_ecs + tsfc*(VCM_Dair + ...
                 VCM_Dphx + VCM_Dshx);
elseif mode≥3 && mode≤8 && LoD(3)≠0 % Flying normally
    % [kg/s] Fuel consumption of ECS circulation fans and weight penalty
    E_VCM_Fuel = kp*tsfc*shaftpower_VCM_ecs + tsfc*(VCM_Dair + ...
                 VCM_Dphx + VCM_Dshx) - ...
                 tsfc*g*(Mass_ECS_Conv - Mass_ECS_E_VCM)/LoD(3);
elseif mode≥3 && mode≤8 && LoD(3)==0% Flying with no lift
    % [kg/s] Fuel consumption of ECS circulation fans
    E_VCM_Fuel = kp*tsfc*shaftpower_VCM_ecs + tsfc*(VCM_Dair + ...
                 VCM_Dphx + VCM_Dshx);
else % Statis on ground. Connected to ground power.
    E_VCM_Fuel = 0;
end
```

For DIVA

{
"Author1": { "name": "Emil Holmgren"},
"Author2": { "name": "Dhruv Haldar"},
"Degree": {"Educational program": "Master's Programme, Aerospace Engineering, 120 credits"},
"Title": {
"Main title": "More Electric Aircraft (MEA)",
"Subtitle": "Scaling aspects and Weight impact",
"Language": "eng" },
"Alternative title": {
"Main title": "Mer Elektriskt Flyg",
"Subtitle": "Skalningsaspekten och Viktpåverkan",
"Language": "swe"
},
"Supervisor1": { "name": "Andreas Johansson, andreas.x.johansson@saabgroup.com" },
"Examiner": {
"name": "Lina Bertling Tjernberg, linab@kth.se",
"organisation": {"L1": "School of Electrical Engineering and Computer Science" }
},
"Other information": {
"Year": "2021", "Number of pages": "xvii,71"}
}